LONGITUDINAL VORTICES DEVELOPING IN A PLANE STRAIN FIELD

J. Wu[a], J Sheridan[b], M. Welsh[a] and K. Hourigan[a]
[a] Division of Building, Construction and Engineering, CSIRO, Highett 3190, Australia
[b] Department of Mechanical Engineering, Monash University, Clayton 3168, Australia

ABSTRACT

In this paper, an ideal three-dimensional vortex filament is introduced into a plane strain field and its time evolution has been simulated in the Lagrangian frame of reference. It is demonstrated that a localised perturbation, consisting of a small displacement of the vortex filament, spreads across the span of the filament to form a wave-type pattern. The 'waves' are further stretched due to the background velocity of the plane strain field to form counter-rotating longitudinal vortices. Flow visualisations were conducted to examine the plane strain field formed in the stagnant region of flow impinging on a flat plate placed in a cross-flow.

INTRODUCTION

It has been recognised in recent years through the works of Wei and Smith (1986), Williamson (1988), Welsh *et al.* (1992), Bays-Muchmore and Ahmed (1993) and Wu *et al.* (in press) that longitudinal vortices develop in the wake of bluff bodies. They are found to be flow structures consisting of pairs of inclined counter-rotating vortices. Similar three-dimensional vortical structures have been shown to exist in plane mixing layers by Bernal and Roshko (1986), among others.

It is generally agreed that the longitudinal vortices result from an instability of the base flow; the base flow is the vortex street in wakes or spanwise rollers due to the Kelvin Helmholtz instability in mixing layers. However, the process whereby longitudinal vortices are formed is still an open question and remains to be solved. Lin and Corcos (1984) studied unidirectional vorticity along the direction of positive strain of a plane strain field. The evolution process is found to be controlled by the mutual and self-induction of the vorticity and the stretching of the background plane strain field.

In this paper, the plane strain field model of Lin and Corcos is further investigated using an ideal three-dimensional vortex filament method based on the inviscid vortex dynamics theory. Flow visualisation experiments were conducted to examine the flow structures developing in a plane strain field.

VORTEX FILAMENT SIMULATION

Vortex dynamics

The Biot-Savart equation can be used to calculate velocity field induced by a vorticity field. The Biot-Savart equation is singular at the centre of the vortex filament if the filament curvature is non-zero (Batchelor 1967). In reality, the finite size of the core of the filament and diffusion (molecular and turbulent) tend to smooth the singularity, therefore a cut-off function is needed to eliminate the singularity. Leonard (1985) recommended a Rosenhead-Moore approximation:

$$\frac{\partial \mathbf{r}_i}{\partial t} = -\sum_{j=1}^{N} \frac{\Gamma_j}{4\pi} \int \frac{(\mathbf{r}_i(s,t) - \mathbf{r}_j(s,t)) \times (\partial \mathbf{r}_j/\partial s) ds}{(|\mathbf{r}_i - \mathbf{r}_j|^2 + \alpha\sigma^2)^{3/2}} \tag{1}$$

where $\mathbf{r}_j(s), j = 1, 2, ...N$ are space curves for N filaments (the left side is the advective velocity induced by self/mutual interactions of N vortex filaments), σ is a core size parameter which depends on s and t, α is a model coefficient and is chosen as 0.22 to yield the correct speed for a ring vortex, s is a coordinate fixed on the filament curve, and t is time. In the current simulation only a single vortex filament is considered, hence $N = 1$. The circulation Γ_j of the filament can be treated as a constant in simulations, in accordance with Kelvin's law.

Computation of vortex filament evolution

A computer code has been developed which calculates the evolution of a single vortex filament introduced into the background plane strain field as shown below.

$$\begin{aligned} U_x &= xk \\ U_y &= -yk \\ U_z &= 0, \end{aligned} \tag{2}$$

where U_x, U_y and U_z are velocity components in the x, y and z direction respectively, and k is the strain rate. The computation steps include:
1) The base flow field, i.e. the plane strain field described by (2) is calculated and stored.
2) A filament, discretised into linear segments, is introduced into the base flow.
3) The self-induced velocity of each segment is calculated.
4) The advective velocity of each segment is found:

$$\mathbf{V} = \mathbf{V}_{base} + \mathbf{V}_{self} \tag{3}$$

where $\mathbf{V}$ denotes velocity vector, the subscripts *base* and *self* denote the velocities due to the base flow and self-induced velocity of the filament, respectively.
5) The filament elements are advected using a predictor-corrector scheme:

$$\mathbf{r}' = \mathbf{r}_t + \mathbf{V}\Delta t$$

$$\mathrm{V}' = \mathrm{V}_{base}(\mathrm{r}') + \mathrm{V}_{self}(\mathrm{r}') \tag{4}$$
$$\mathrm{r}_{t+\Delta t} = \mathrm{r}_t + \frac{(\mathrm{V} + \mathrm{V}')}{2}\Delta t$$

here $\mathbf{r}_t$ and $\mathbf{r}_{t+\Delta t}$ are the position vectors of the filament segment at time t and $t + \Delta t$ respectively, the superscript $(')$ denotes an intermediate step.

Step 3 to step 5 are repeated until the completion of the calculations.

Due to the stretching of the filament, the segment length of the discretised filament increases rapidly. To overcome this problem, extra nodes are introduced at each time step to maintain sufficient spatial resolution.

Vortex filament evolution in a plane strain field

The parameters used for simulation are listed in Table 1, where Γ^* and t^* are normalised circulation and time respectively, σ_0 is the initial vortex core diameter, and k is the strain rate.

Table 1: Parameters for simulation of a vortex filament in a plain strain field.

Computing Parameters	
number of initial nodes n_0	100
number of final nodes n_e	200
strain rate k	4
time-step $\delta t^* = \delta t k$	0.008
simulation period $t^* = tk$	4.24
vortex strength $\Gamma^* = \Gamma/(\sigma_0^2 k)$	62.5
vortex core size σ_0/a	0.02

A straight line vortex filament with a uniform core size is initially introduced into the two-dimensional plane strain field, at position '1' (Fig. 1(a)). The streamline pattern of the plane strain field is plotted at a section $z = z_0 = 5$ in the xy-plane. The strain field as characterised by (2) is identical along the z-axis. A localised disturbance consisting of a small displacement of the vortex filament is applied at the middle of the span of the filament. The amplitude of the disturbance has a Gaussian distribution, and its maximum amplitude is approximately equal to the vortex core diameter.

Figure 1(a) shows a perspective view of the three-dimensional time evolution of a single vortex filament in the strain field. The vortex filament is initially introduced at position '1'; and the perturbation is applied at the middle span of the filament ($z = 5$). The locally perturbed vortex filament progressively deforms into a wave-like vortex loop on arriving at position '2' due to the combined action of the self-induction and background stretching effect of the plane strain field. The background plane strain field is invariant along the z-axis; its streamline pattern (the xy-plane) is also included in the perspective view at $z = 5$. Figure 1(b) is a view in the xy-plane showing how the vortex filament

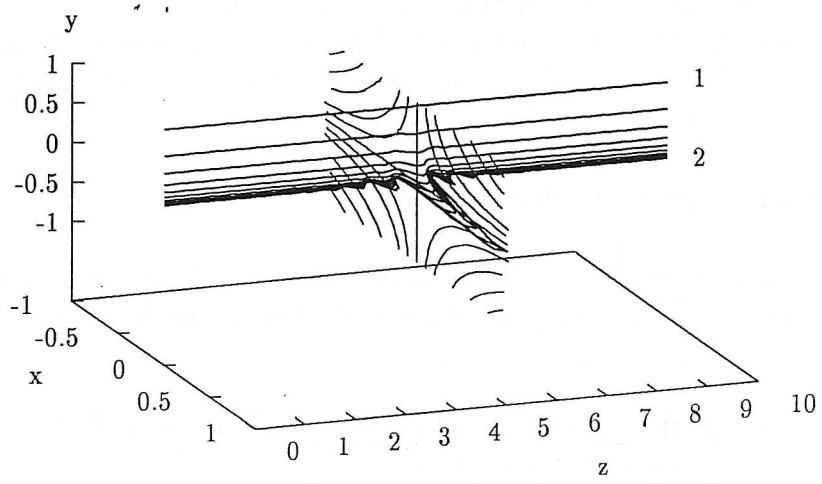

(a)

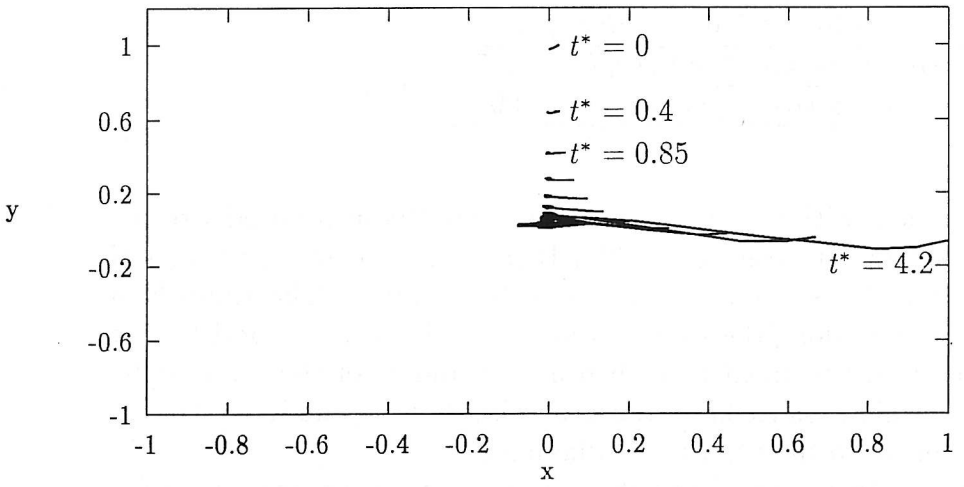

(b)

Figure 1: Vortex filament evolution in a plain strain field, $\Gamma^* = 62.5$, initial position '1': $t^* = 0$, final position '2': $t^* = 4.24$: (a) a perspective view, the streamline pattern of the plane strain field is plotted at $z = 5$ to indicate the spatial position the filaments advected through; (b) xy-plane view.

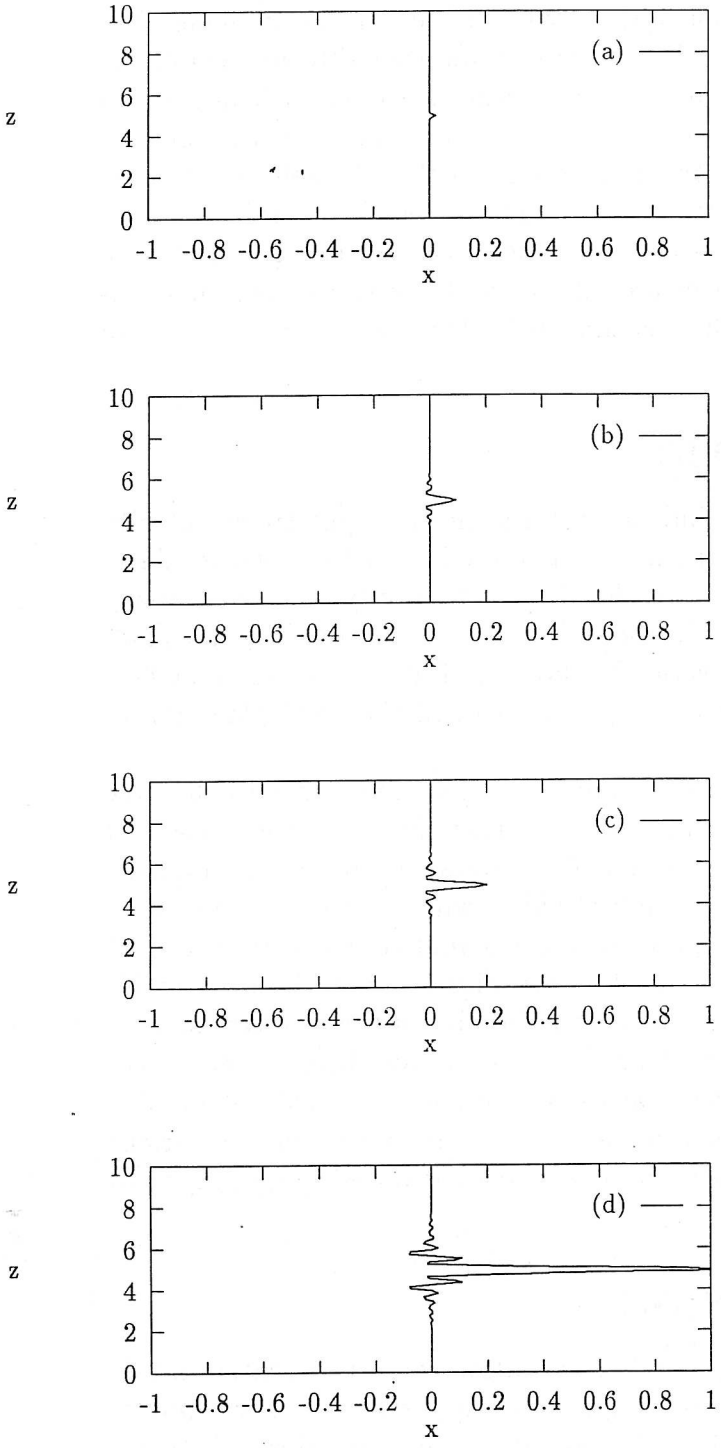

Figure 2: Snapshots of a vortex filament time-evolution in a plain strain field $\Gamma^* = 62.5$, xz-plane view: (a) $t^* = 0$, (b) $t^* = 1.7$, (c) $t^* = 2.5$, (d) $t^* = 4.24$.

evolves into elongated loops aligned in the x-direction or the positive axis of the strain field.

Figure 2 shows snapshots of time-evolution of the vortex filament in the xz-plane. The disturbance, initially with a Gaussian shape, in time transmits 'waves' to its neighbourhood. The formation of the wavy pattern, due to the spread of the disturbance across the filament span, is caused by the self-induction of the vorticity field. The wave growth is intensified by the background stretching from the strain field. The self-induction is enhanced when the amplitude of the wave is increased. Therefore, the overall evolution process is associated with the combined effects of induction and stretching. Clearly an array of counter-rotating longitudinal vortices are set up in this way and are superimposed on the nominally two-dimensional plane strain field. The vortices are aligned in the positive strain direction.

EXPERIMENTAL OBSERVATION

Flow visualisation was conducted in a low turbulence water tunnel at a freestream velocity of 0.274 m/s. The longitudinal turbulence intensity, calculated from the hot-wire data, is typically 0.1%. The spectrum of the fluctuating longitudinal velocity was free of sharp peaks and decreased in amplitude by 20 dB/Hz above 0.08 Hz. A 129 mm long flat plate was placed normal to the freestream flow direction as shown in Fig. 3. The stagnant flow field outside the boundary layer can be used to represent half of the ideal plane strain field studied by the vortex filament method.

Hydrogen bubbles generated by a cathode nicrome wire were released into the flow downstream of the stagnation point; a laser light sheet perpendicular to the surface of the plate was used to illuminate a cross-flow section 20 mm downstream of the stagnant point. The flow pattern was recorded using a standard video camera. The flow visualisation configuration and typical observed flow patterns are schematically drawn in Fig. 3. Still photographs digitised from the video tape are shown in Figs 4(a) and (b) at two arbitrary time instants. The mushroom type structures are indicative of the counter-rotating vortices aligned in the diverging flow direction along the body surface. Upon careful scrutinising of the video sequence, it was concluded that the vortices were formed well outside the boundary layer, and the centre of the vortices were 4 or 5 mm away from the surface of the plate. It was also observed that the position of the vortices varied irregularly with time.

DISCUSSION AND CONCLUSION

Based on the vortex filament simulations and flow visualisation results presented in this paper, it can be stated that a plane strain field is capable of supporting the development of pairs of counter-rotating vortices aligned in the positive strain direction. A three-dimensional vorticity tube is fundamentally unstable and can evolve into a wave-type pattern due to the spread of the disturbance across the span of the vortex filament.

It is proposed that the evolution of a three-dimensional vortex filament in the plane strain field can be used as a model to explain the formation of the counter-rotating

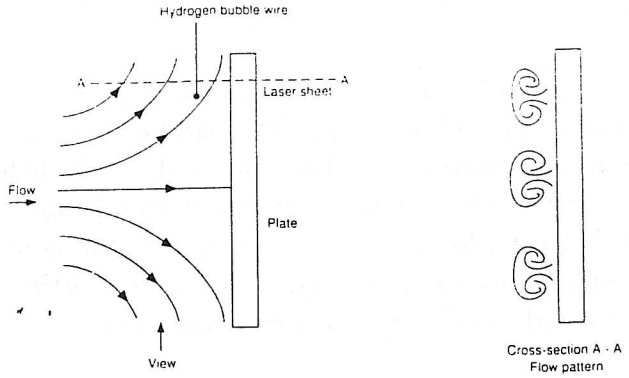

Figure 3: Flow visualisation experimental set-up.

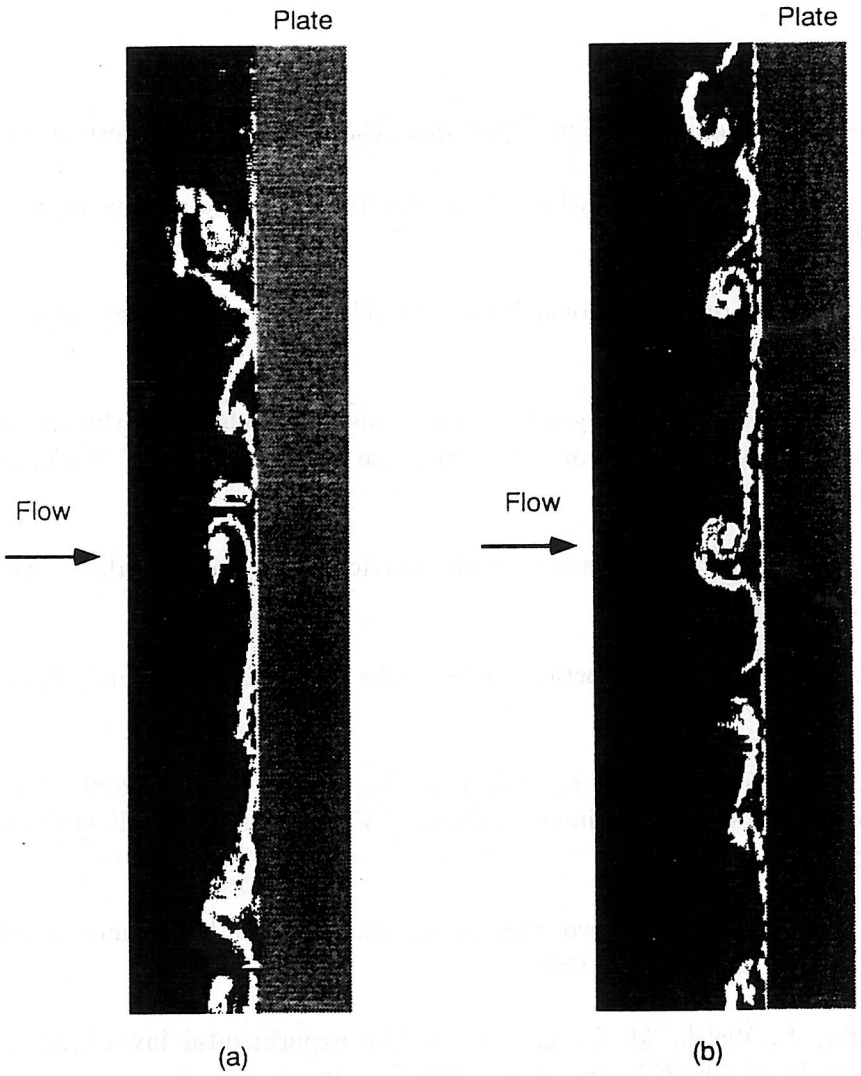

Figure 4: Longitudinal vortices formed near the stagnation region of flow impinging on a plate: (a) instant 1, (b) instant 2.

longitudinal vortices developing in shear flows (e.g. wakes, mixing layers and jets). For example, in the case of the wake behind bluff bodies, the saddle point region (Wu *et al.* in press) formed by the Strouhal vortices produces a local strain field similar to the one discussed here. Spanwise vorticity tubes approaching the saddle point region would then develop into distorted vortex loops and hence generate the counter-rotating longitudinal vortices. This corresponds to the observation that these vortices are aligned in the stretching direction in the braids joining the spanwise vortices.

ACKNOWLEDGMENTS

The authors acknowledge the support from an Australia Research Council grant. J. Wu wishes to acknowledge the support from a Monash University Scholarship.

REFERENCE

Batchelor, G. K., 1967, '*An Introduction to Fluid Dynamics*', Cambridge Univ. Press, p. 615.

Bernal, L. P. and Roshko, A., 1986, 'Streamwise vortex structure in plane mixing layers', *J. Fluid Mech.*, **170**, 499-525.

Leonard, A., 1985, 'Computing three-dimensional incompressible flows with vortex elements', *Ann. Rev. Mech.*, **17**, 523-559.

Lin, S. J. and Corcos, G. M., 1984, 'The mixing layer: deterministic models of a turbulent flow. Part 3. The effect of plane strain on the dynamics of streamwise vortices', *J. Fluid Mech.*, **141**, 139-178.

Bays-Muchmore, B. and Ahmed, A., 1993, 'On streamwise vortices in turbulent wakes of cylinders', *Phys Fluids*, A **5**(2), 387-392.

Wei, T. and Smith, C.R., 1986, 'Secondary vortices in the wake of circular cylinders', *J. Fluid Mech.*, **169**, 513-533.

Welsh, M. C., Soria, J., Sheridan, J., Wu, J., Hourigan, K., Hamilton, N., 1992, 'Three-dimensional flows in the wake of a circular cylinder', *Album of Visualization, The Visualization Society of Japan*, **9**, 17-18.

Williamson, C. H. K., 1988, 'The existence of two stages in the transition to three-dimensionality of a cylinder wake', *Phys Fluids*, **31**(11) 3165-3168.

Wu, J., Sheridan, J., Soria, J., Welsh, M. C., (in press), 'An experimental investigation of streamwise vortices in the wake of a bluff body', *J. Fluid & Structures.*